Title:

A novel allele of *Mitogen Activated Protein Kinase 6* is linked to disease resistance and constitutive immunity in rice.

Authors:

Gokulan C.G.[1,6,†], Mohammed Jamaloddin[1,†], Deepti Rao[1], Namami Gaur[1,2], Amita Rani Supriyo[1], Nisha Sao[1], Deepak Niranjan[1,7], Shrish Tiwari[1], Gouri S. Laha[3], Kalyani M. Barbadikar[3], Raman Meenakshi Sundaram[3], Sheshu Madhav Maganti[3,4,*], Hitendra K. Patel[1,5,*], Ramesh V. Sonti[1,7,*]

Affiliations:

[1]CSIR-Centre for Cellular and Molecular Biology, Telangana, India.

[3]ICAR-Indian Institute of Rice Research, Telangana, India.

[5]Academy of Scientific and Industrial Research, Uttar Pradesh, India.

[†]These authors should be considered joint first author.

[*]Addresses for correspondence: Sheshu Madhav Maganti - sheshu24@gmail.com; Hitendra K. Patel - hkpatel@ccmb.res.in; Ramesh V. Sonti – rameshvsonti@gmail.com

Present addresses:

[2]The James Hutton Institute, University of Dundee, Scotland.

[4]ICAR-Central Tobacco Research Institute, Andhra Pradesh, India.

[6]Centre for DNA Fingerprinting and Diagnostics, Telangana, India.

[7]International Centre for Genetic Engineering and Biotechnology, New Delhi, India.

Word count: 6614

SUMMARY

Bacterial Blight (BB) is the most serious bacterial disease of rice. Usage of resistant cultivars has been a successful strategy in controlling BB. However, constant selection pressure causes the evolution of hypervirulent pathogenic strains that break down resistance, thus necessitating additional sources of resistance. An induced-mutant line derived from the elite rice cultivar Samba Mahsuri was identified to exhibit broad-spectrum resistance to BB. Using next-generation gene mapping approaches, we identified a genomic interval in chromosome 6 to be linked to BB resistance. Analysis of the SNPs in the locus and subsequent linkage analysis indicated that a missense SNP located in the second exon of the *Mitogen-Activated Protein Kinase 6* (*OsMAPK6*) could be the causal mutation. A detailed examination of *OsMAPK6* gene sequences in over 4000 rice genomes revealed that the mutant allele identified in this study is novel to rice germplasm. The candidate SNP causes the substitution of an invariant Serine residue with a Proline residue (S84P), thus likely affecting the protein function. Global transcriptome, metabolome, biochemical, and molecular analyses suggested that BB42 exhibit constitutive immunity. On the mechanistic front, the mutation seems to result in diminished brassinosteroid signaling in BB42. Taken together, we report a novel allele of a highly conserved *MAPK* gene and provide evidence for its possible association with constitutive immunity and disease resistance in rice.

KEYWORDS: Bacterial blight, Disease resistance, Gene mapping, MAP kinase, Plant immunity, Rice, *Xanthomonas*.

INTRODUCTION

Plants possess a potent innate immunity which every cell that faces a threat can elicit. The two-tiered innate immunity of plants consists of Pattern-Triggered Immunity (PTI) and Effector-Triggered Immunity (ETI) (Jones and Dangl, 2006). PTI is elicited by the recognition of the Pathogen-Associated Molecular Patterns (PAMPs) or Damage-Associated Molecular Patterns (DAMPs). PAMPs include conserved microbial-derived molecules like flagellin, peptidoglycan, LPS, and chitin; DAMPs include damage-associated molecules like extracellular ATP, extracellular DNA, and oligogalacturonides (Chen and Ronald, 2011; Pontiggia *et al.*, 2020). The patterns are perceived by the membrane-bound receptor kinases, that are collectively called as Pattern Recognition Receptors (PRRs), that relay signals to the signaling proteins like the MITOGEN-ACTIVATED PROTEIN KINASE (MAPK), that typically transduce the signals to transcription factors. PTI induces an extensive transcriptional and translational reprogramming that results in the production of defense-related proteins, phytohormones, and metabolites, thus limiting pathogen entry and proliferation (D Couto, 2016; Yuan *et al.*, 2021; Zipfel and Felix, 2005). On the other hand, ETI is a stronger defense response that is activated by the recognition of pathogen-secreted proteins (also known as effectors) by intracellular receptors mainly belonging to the Nucleotide-Binding and Leucine-rich Repeat containing Receptors (NB-LRRs/NLRs) superfamily. ETI is manifested by the Hypersensitive Response (HR) which results in a localized cell-death, thus restricting the spread of pathogens (Jones *et al.*, 2016). On the other hand, uncontrolled regulation of various arms of the plant immune system results in constitutive immunity which in turn results in various traits like stunted growth, spontaneous lesions, and disease resistance among others (Freh *et al.*, 2022).

Bacterial Blight (BB) is the most serious bacterial disease of rice that can result in up to 70% yield loss depending on the infection severity (Goto, 1992; K. Reddy, 1979; Ou, 1973, 1985). Rice cultivation in India is affected by BB with ~8.5% loss in annual yield (Savary *et al.*, 2019). BB is caused by the Gram-negative bacterium *Xanthomonas oryzae* pv. *oryzae* (*Xoo*). *Xoo* invades rice leaves through hydathodes and colonizes the extracellular spaces in xylem parenchyma tissue (Hilaire *et al.*, 2007). Under high humidity conditions, the bacteria ooze out of the openings such as hydathodes or wounds and form beads or strands of exudates that potentially act as inoculum for further infections (Mew, 1993). Being a prolific colonizer of the vascular tissue, *Xoo* spreads systemically along the veins and results initially in chlorotic yellow and later in necrotic lesions

74 on the infected leaves, ultimately leading to drying of the leaves (Joshi *et al.*, 2020; Niño-Liu *et*
75 *al.*, 2006)**.**

76 Previous studies have associated several genes and their alleles with BB resistance, of
77 which a few alleles are widely used in breeding programme to develop BB resistant rice varieties
78 (Fiyaz *et al.*, 2022; Jamaloddin *et al.*, 2021; Jiang *et al.*, 2020). Such resistant varieties have been
79 deployed in the field with ample success (Dasari *et al.*, 2022; Huang *et al.*, 1997; Jamaloddin *et*
80 *al.*, 2020; Oliva *et al.*, 2019; Pradhan *et al.*, 2015; Sundaram *et al.*, 2008). It was observed that a
81 combination of two to three *R*-genes was effective against majority of the *Xoo* pathotypes.
82 However, a constant selection pressure on pathogens combined with their rapid generation time is
83 expected to result in the evolution of adapted pathotypes that breakdown existing sources of
84 disease resistance. Studies have identified multiple strains of *Xoo* that breakdown individual
85 resistance genes (Kaur *et al.*, 2020; Mishra *et al.*, 2013; Quibod *et al.*, 2020; Yugander *et al.*, 2017,
86 2022). Adding another layer to this serious issue is the migration of hypervirulent strains from one
87 country to another (Carpenter *et al.*, 2020). Despite the existence of several *R*-genes, the practical
88 deployment of the genes needs to be rigorously tested on a case-to-case basis to ensure the
89 compatibility of the genes to different agroclimatic zones. For instance, although *Xa7* was
90 identified to be a broad-spectrum R-gene, a study in India found that 94% of the 71 strains tested
91 were virulent on a *Xa7*-positive rice line (Yugander *et al.*, 2022). Therefore, to counter resistance
92 gene breakdown and to curb disease outbreaks, it is essential to identify new sources of broad-
93 spectrum resistance that are suitable for given agroclimatic conditions and the cultivar background.

94 Mutation breeding is an efficient method to obtain novel sources of resistance in relatively
95 less time, while preserving the genetic architecture of the desired cultivar. Further, the availability
96 of advanced gene mapping approaches enables forward genetics using populations derived from
97 the induced mutant lines (Abe *et al.*, 2012; Takagi *et al.*, 2013). Earlier, we reported the generation
98 and screening of a large-scale ethyl methanesuphonate-induced mutant lines of the rice mega-
99 variety Samba Mahsuri for various traits of economic importance (Potupureddi *et al.*, 2021). Here,
100 we report the characterization of one of the mutant lines (henceforth BB42) that exhibited a broad-
101 spectrum resistance to various hypervirulent isolates of *Xoo*. Through a genetic mapping study,
102 we observed that resistance in BB42 is controlled by a single recessive locus. We further identified
103 a SNP located in the second exon of *OsMAPK6* gene that causes Serine to Proline substitution at
104 the 84th position and cosegregates with the resistance trait. Notably, the mutant allele identified

105 here represents a novel genetic variation in the rice germplasm. Transcriptome profiling in
106 combination with multiple biochemical and molecular assays revealed a constitutively active basal
107 defense signaling in BB42 when compared to SM. Particularly, several kinase-encoding genes
108 were significantly upregulated, and several members of the major transcription factor families
109 were differentially expressed. Overall, our study reports a novel allele of *OsMAPK6* that is linked
110 to bacterial blight resistance, and constitutive immunity and presents a potential genetic source for
111 breeding BB resistance in rice.

112 **RESULTS**

113 **BB42 exhibits broad-spectrum resistance to highly virulent *Xoo* isolates**

114 Earlier, we identified BB42 from an EMS-induced mutant library of SM as a line exhibiting
115 enhanced resistance to the bacterial blight disease of rice (Potupureddi *et al.*, 2021). Here, we
116 characterized BB42 further through a combination of phenotyping, genomic, molecular,
117 transcriptomics and metabolomics approaches. Morphologically, BB42 exhibited reduced height
118 compared to SM (Fig. 1A, B). Further, to understand the spectrum of resistance, we challenged
119 BB42 with several hypervirulent strains of *Xoo* that were shown to breakdown resistance provided
120 by major resistance genes including *xa5*, *xa13* and *Xa21* (Mishra *et al.*, 2013). The results revealed
121 that BB42 exhibits enhanced resistance to all the tested *Xoo* strains (Fig. 1C, D). Notably,
122 challenging SM and BB42 with *Xanthomonas oryzae* pv. *oryzicola* (*Xoc*) – a pathovar of *X. oryzae*
123 that causes bacterial leaf streak (BLS) in rice - showed no difference in the susceptibility.
124 Intriguingly, the susceptibility level of SM to *Xoc* was significantly lesser than that of Nipponbare
125 - another BLS susceptible rice variety (Figure S1A). Taken together, these results suggest that
126 BB42, a semi-dwarf mutant of SM, is resistant to *Xoo* in what appears to be a non-race-specific
127 manner.

128 **A missense mutation in *OsMAPK6* is linked to bacterial blight resistance**

129 We next aimed to identify the genetic basis of bacterial blight resistance in BB42. To this
130 end, we generated two F_2 populations, each with 244 plants, and screened them with a virulent
131 *Xoo* strain, IXO1221. Phenotype segregation in both the populations followed the Mendelian ratio
132 for a monogenic recessive trait (Table S4; Figure S2A, B). Progenies from both the populations
133 were used for gene mapping through the QTL-sequencing pipeline (Takagi *et al.*, 2013). The
134 analysis revealed a genomic interval in the short arm of chromosome 6, in both the populations, to

135 be linked to resistance (Fig. 2A, B). We identified five Single Nucleotide Polymorphisms (SNPs)
136 within the interval, of which, one SNP was annotated as a 'missense and splice region' variant and
137 was predicted to be deleterious (Table 1). This SNP (T → C at SM-Chr6:2664062) is located in
138 the second exon of the rice *Mitogen Activated Protein Kinase 6* (*OsMAPK6*) gene and results in
139 the substitution of a Serine by Proline (Fig. 2C). Analysis of the RNA reads mapped to OsMAPK6
140 indicated no anomalies in the splicing of the gene between SM and BB42 (Figure S3). Multiple
141 sequence alignment of one-hundred MAPK6 homologues across different plant species indicated
142 a 100% conservation of the affected Serine residue (Fig. 2D). Notably, when searched in the
143 RiceVarMap V2.0 database (Zhao *et al.*, 2021) which contains sequences of about 4500 rice
144 accessions, we found no accession to carry any variation at this position. To further ascertain the
145 co-segregation of the observed SNP with BB resistance, we developed PCR-based markers that
146 differentiate the SM and the BB42 alleles (Figure S2C). We tested randomly selected F_2 progenies
147 that were resistant or susceptible to *Xoo* IXO1221 and found that the BB42 allele of *OsMAPK6*
148 co-segregated with the resistant progenies, whereas the susceptible progenies were homozygous
149 for SM allele or were heterozygous (Fig. 2E). Overall, these results suggest that the variation in
150 the *OsMAPK6* gene likely confers BB resistance. The identified allele is novel to rice germplasm
151 and the affected Serine residue is evidently invariable in MAPK6 homologues that were assessed,
152 indicating a likely role of this novel variant in BB resistance.

153 ***Xoo* induces an overlapping transcriptome change in SM and BB42**

154 Given the central role of MAPK6 in orchestrating cellular signalling during defense and
155 development, we reasoned that BB42 and SM are likely to have different transcriptional profiles
156 which might explain the observed resistance to *Xoo*. Therefore, we performed a global
157 transcriptome profiling of leaves from SM and BB42 that were sampled immediately post infection
158 (Mock) or at 24 hours post infection with *Xoo* IXO1221 (*Xoo*). The samples were analysed to
159 identify the treatment-based transcriptome changes in both the genotypes (i.e., *Xoo* vs Mock in
160 SM and BB42) as well as genotype-specific transcriptome differences in both the treatments (i.e.,
161 BB42 vs SM in Mock and *Xoo*). Four combinations of samples were analysed in total and the
162 results indicated that *Xoo* treatment caused a major transcriptome reprogramming in both the
163 genotypes (1974 DEGs in SM and 1477 DEGs in BB42) (Data S1). On the other hand, the
164 genotype-specific differences in the transcriptome were relatively smaller (810 DEGs in Mock

165 treatment and 493 DEGs in *Xoo* treatment) (Fig. 3A; Figure S4; Table S5). Further comparative
166 analyses revealed that about 60% of the upregulated genes in SM and BB42 upon *Xoo* infection
167 were common (Fig. 3B). With regards to the downregulated genes, about 87% of the genes
168 downregulated in BB42 were also downregulated in SM upon *Xoo* infection (Fig. 3B), while
169 several additional genes were uniquely downregulated in SM. This is suggestive of a largely
170 similar *Xoo*-mediated transcriptional landscape in SM and BB42 at gene level, which is also
171 reflected at pathway levels (Figure S5).

172 We then performed a *k*-means clustering analysis of the top 2000 genes exhibiting highly
173 variable expression across different samples and treatments. We observed 1628 genes showing
174 similar expression trend in both SM and BB42, whereas 372 genes showed an increased expression
175 in BB42 irrespective of the treatment, when compared to SM (Fig. 3C; Cluster B). Intrigued by
176 this observation, we did a cluster-wise GO term enrichment analysis and noted that cluster B was
177 enriched with genes that are involved in defense response and cell signalling. It is mention-worthy
178 that the higher expression of defense genes is observed even in control BB42 plants (Fig. 3C),
179 which points towards the likelihood of a constitutively active defense in BB42. Therefore, we
180 probed deeper to understand the nature of constitutive defense in BB42 using DEGs from the
181 mock-treated samples.

182 **BB42 exhibits constitutive immunity**

183 We considered the DEGs between mock-treated BB42 and SM for further analysis to
184 understand the basal genotype-specific differences. A GO term enrichment analysis revealed
185 higher expression levels of genes involved in defense response, receptor signalling, and protein
186 phosphorylation (Fig. 4A). Conversely, certain genes involved in wounding response, response to
187 jasmonic acid, and regulation of transcription were expressed at lower levels in BB42 in
188 comparison to SM (Fig. 4A). We first looked into the genes present in the highly expressed
189 categories and noted the presence of various classes of defense related genes (n=41) encoding
190 receptor kinases, receptor-like cytoplasmic kinases, a catalase, pathogenesis-related proteins and
191 a JA biosynthetic protein (Table S6). Very importantly, amongst the above set of genes were
192 fourteen genes encoding Nucleotide-Binding adaptor shared by APAF-1, R proteins, and CED-4
193 (NB-ARC) domain containing proteins and Nucleotide-Binding Leucine-rich Repeat containing
194 Receptor proteins (NB-LRR or NLRs), which is one of the characteristic traits observed in

195 autoimmune mutants in plants (Freh *et al.*, 2022) (Figure S6). While this suggests an enhanced
196 defense signalling in BB42, we were puzzled to observe downregulation of JA responsive genes.
197 However, a detailed inspection indicated that such genes encoded the JASMONATE-ZIM
198 DOMAIN (JAZ or TIFY) proteins, which act as repressors of JA signalling (Table S7). This further
199 suggests the possibility of an active and/or enhanced JA signalling in BB42. To validate this
200 observation and also to check if this scenario persists through different developmental stages, we
201 performed quantitative PCR using defense marker genes (PR genes) in SM and BB42 seedlings.
202 In accordance with the previous observation, we found significant upregulation of defense marker
203 genes in BB42 seedlings (Figure S76A). Moreover, we found other hallmarks of defense activation
204 like H_2O_2 accumulation and MAPK activation to be enhanced in BB42 even in unelicited
205 conditions (Figure S7B, C). Further, as we observed an upregulation of various types of kinases,
206 we used Phospho-Serine and Phospho-Threonine/Tyrosine antibodies to assess the qualitative
207 differences in the phosphorylated proteins in SM and BB42. There was an observable difference
208 in the signal patterns in all forms of phosphorylated proteins between SM and BB42 (Figure S7D).
209 By and large, the transcriptomics data in combination with other assays and the dwarf stature of
210 BB42 are indicative of constitutive immunity and a differential phosphorylation-mediated
211 signalling between the two lines.

212 We performed an untargeted metabolite profiling of SM and BB42 leaves at the tillering
213 stage and observed a general difference in the metabolite profiles of SM and BB42 (Figure S8A).
214 Among the detected metabolites, 92 metabolites were differentially accumulated (DAMs), of
215 which 40 were relatively abundant in BB42 and 52 were relatively abundant in SM (Figure S8B;
216 Data S2). Enrichment analysis of the DAMs indicated linoleic acid metabolism, vitamin B6
217 metabolism, and nicotinate metabolism to be upregulated and starch and sucrose metabolism, and
218 glutathione metabolism to be downregulated in BB42 (Figure S9). On that note, levels of some of
219 the compounds associated with the above pathways showed clear difference between SM and
220 BB42. Notably, compounds that are associated with defense like linoleic acid and coniferaldehyde
221 were abundant in BB42, while compounds that were associated with disease susceptibility like
222 sucrose, *trans*-Zeatin, and amino acids were abundant in SM (Fig. 4B).

223

224

225 **Brassinosteroid signalling is affected in BB42**

226 Earlier, Liu *et al.*, (2015) identified an allele of *OsMAPK6* that resulted in dwarf stature
227 and small grain size (*dsg1*) and showed that the observed traits were due to imbalance in
228 brassinosteroid (BR) homeostasis. Interestingly, analysis of various morphological traits showed
229 slight similarity between *dsg1* and BB42. For instance, BB42 grains were slightly yet significantly
230 shorter than those of SM, but there were no difference in grain width (Fig. 5A, B, C). We then
231 tested the BR sensitivity of SM and BB42 plants by measuring coleoptile elongation following
232 treatment with 24-epibrassinolide (epiBL). The elongation of BB42 coleoptile in response to
233 epiBL was not as significant as that of SM, suggesting a reduced sensitivity to BR in BB42 (Fig.
234 5D). Intriguingly, brassinolide was detected in the metabolome profiling and its level was slightly,
235 albeit not significantly, higher in BB42 than in SM (Fig. 5E). It is possible that the reduced
236 sensitivity to BR in BB42 might have negatively impacted the feedback inhibition of BR
237 biosynthesis, thus resulting in higher basal BR levels. Additionally, expression of several genes
238 involved in BR signalling and response was diminished in BB42 as compared to SM (Table S8).
239 On the whole, it seems like BB42 is impaired in BR sensitivity and a role of the mutated
240 OsMAPK6 in this impairment could be speculated.

241 **DISCUSSION**

242 In this study, we report an EMS-induced allele of *Mitogen-Activated Protein Kinase 6* and
243 show its involvement in resistance to bacterial blight, which is a serious disease of rice. The variant
244 of OsMAPK6 identified here is new to rice germplasm wherein an otherwise invariant Serine at
245 the 84th position is replaced by Proline. Not just in plants, the affected Serine was observed to be
246 invariant in MAPK6 homologues of different kingdoms (Figure S10A, B). Further, the serine
247 residue is conserved in ten of the seventeen rice MAPKs (Figure S11A, B). These results signify
248 the importance of the Serine residue for the function of MAPK6 homologues and perhaps in
249 majority of the rice MAPKs as well. The causal SNP is a T to C transition, a non-canonical type
250 of EMS-induced variation. EMS is believed to predominantly cause G/C to A/T type transitions,
251 although exceptions are reported (Abe *et al.*, 2012; Greene *et al.*, 2003; Jhingan *et al.*, 2023;
252 Loveless, 1969; Till *et al.*, 2007).

253

254 **Effect of the variation on MAPK6 function**

255 MAPK6 homologues are highly conserved across eukaryotes and play vital roles in disease
256 and development (Meng and Zhang, 2013; Sun and Zhang, 2022). Previous studies have associated
257 OsMAPK6 with various growth processes (Liu *et al.*, 2015; Xu *et al.*, 2018; Yi *et al.*, 2016) as
258 well as defense response and resistance to diseases like blast, blight and bacterial leaf streak (Chen
259 *et al.*, 2021; Chujo *et al.*, 2014; Kim *et al.*, 2012; Kishi-Kaboshi *et al.*, 2010; Lieberherr *et al.*,
260 2005; Xu *et al.*, 2018). It is interesting to note that natural variations in *OsMAPK6* differentially
261 affect the protein activity and resistance to *Xoc* (Ma *et al.*, 2021). In line with this, the observed
262 difference between SM and Nipponbare in their response to *Xoc* (Figure S1A) might be explained
263 by the natural variation in the N-terminus of MAPK6 between SM and Nipponbare (Figure S1B).
264 Further, certain loss-of-function alleles of *OsMAPK6* were reported to cause embryo lethality (Ma
265 *et al.*, 2021; Yi *et al.*, 2016). It was also observed that a heterozygously inherited loss-of-function
266 mutation in OsMAPK6 could confer moderate resistance to *Xoo* and *Xoc* (Ma *et al.*, 2021). Hence,
267 the effect of the S84P mutation on OsMAPK6 function becomes a primary question. The fact that
268 the activation of OsMAPK6 is not affected in BB42 (Figure S6C) suggests that the mutation has
269 not abolished the protein activation and function, rather the protein's function could have been
270 altered. Intriguingly, one of resistant progenies showed a heterozygous genotype in our analysis.
271 Noteworthy, the SNP-index of this variation is not 1.0 in either of the population. This might
272 indicate an effect of the environment, that could have resulted in one or a few heterozygous
273 individuals showing resistance trait getting included in our sequencing and downstream analyses.
274 Nevertheless, none of the susceptible individuals tested were homozygous for the mutant allele
275 and all of the lines that were homozygous for the mutant allele were resistant. On balance, it is
276 possible that the presence of the mutant allele and allele dosage in combination with the
277 environment might contribute to BB resistance.

278 **MAPK6 integrity could be crucial to prevent constitutive immunity in rice**

279 The phenotypes observed in BB42 including dwarf stature and constitutive immunity, seem
280 to partly resemble a defective MAPK cascade reported in the model plant *Arabidopsis thaliana*.
281 In Arabidopsis, three major MAPKs that are involved in plant immunity and pathogen response
282 are AtMPK3, AtMPK4, and AtMPK6 (Sun and Zhang, 2022). Several studies have elucidated the
283 signalling cascade involving AtMPK4 and showed that the MEKK1-MKK1/2/6-MPK4 cascade is

284 involved in the negative regulation of innate immunity (Gao *et al.*, 2008; Lian *et al.*, 2018;
285 Rodriguez *et al.*, 2010). The mutants *mekk1, mkk1/2,* and *mpk4* exhibit stunted growth, severe
286 dwarfism, and enhanced basal defense responses. Subsequent research showed that the MPK4
287 cascade is guarded by NLR proteins SUMM2 and RPS6, which get activated when the cascade is
288 disrupted (Lian *et al.*, 2018; Zhang *et al.*, 2012, 2017). In this context, it is possible that S84P
289 mutation in OsMAPK6 may modify its interactome, which in turn might activate the immune
290 components guarding it.

291 As activation of MAPKs is critical for proper elicitation of plant immunity, the observation
292 of BB42 exhibiting constitutive defense traits which includes MAPK6 activation raises the
293 following question: Is OsMAPK6 activation in unelicited BB42 a cause or consequence of the
294 active defense? A remarkable phenomenon observed in BB42 was the basal upregulation of several
295 NLR-encoding genes, which appears to phenocopy the Arabidopsis plants that express a
296 constitutively active form of MPK3 (CA-MPK3). Studies have revealed that expression of CA-
297 MPK3 causes enhanced expression of NLR encoding genes in a salicylic acid-dependent manner
298 (Genot *et al.*, 2017; Lang *et al.*, 2017, 2022). Expression of CA-MPK3 also resulted in resistance
299 to the bacterial pathogen *Pseudomonas syringae* (Lang *et al.*, 2017). Another study showed that
300 long-lasting activation of MPK3/MPK6 is necessary for ETI-mediated reduction in photosynthetic
301 efficiency in Arabidopsis (Su *et al.*, 2018). In line with this, we observed a reduction in Chlorophyll
302 A in BB42 as compared to SM (Fig. 4B). Further, prolonged activation of MPK3/MPK6 was
303 observed during ETI and such activation was critical for the regulation of SA-responsive genes
304 (Tsuda *et al.*, 2013). This study suggested that the activation duration of MAPK is a determinant
305 of the robustness of immunity. Of note, the consequence of CA-MAPK expression is dependent
306 on the MAPK in question. For instance, overexpression of CA-MPK4 dampened immune
307 responses and abolished pathogen resistance in Arabidopsis (Berriri *et al.*, 2012). Considering the
308 above-discussed points, it is possible that the activation status of the OsMAPK6-S84P variant and
309 NLR expression could be correlated. Nonetheless, the directionality of these two observations is
310 not certain yet. Also, unlike SA in Arabidopsis, our data suggests a possible involvement of JA in
311 the execution of MAPK6-mediated defense responses in rice. Future investigations are needed to
312 draw a firm conclusion.

313 It appears that BB42 is a unique mutant which possesses most hallmarks of autoimmunity
314 except the spontaneous lesions that occur due to localised cell death. In rice, almost all the reported

315 autoimmune mutants display spontaneous lesions on the leaves, thereby earning the name lesion
316 mimic mutants (LMMs); some LMMs show reduced photosynthetic capacity as well (Freh *et al.*,
317 2022; Xiaobo *et al.*, 2020). Interestingly, loss of function mutations in components of MAPK
318 signalling including OsMKK6 and OsMAPK4 have been reported to cause spontaneous lesions
319 and autoimmunity in rice (Jiang *et al.*, 2023; Wang *et al.*, 2021). Although the molecular
320 mechanisms of autoimmunity in rice is still unclear, based on the data presented here, we propose
321 that a module involving MAPK6, NLRs, and JA signalling proteins might govern autoimmunity.

322 **Potential link between MAPK6, BR, and disease resistance**

323 The relationship between OsMAPK6 function and brassinosteroid homeostasis has been
324 established earlier (Liu *et al.*, 2015) and has also been observed in our study (Fig. 5). However,
325 whether the perturbed BR homeostasis has any direct effect on disease resistance remains to be
326 explored. Involvement of BRs in plant-pathogen interaction as well as growth and development
327 has been demonstrated earlier. BRs can act both synergistically and antagonistically with the
328 immune components to regulate growth and defense (Albrecht *et al.*, 2012; Belkhadir *et al.*, 2012;
329 Heese *et al.*, 2007; Liao *et al.*, 2020). In rice, BRs were shown to suppress rice immunity against
330 a root pathogen (De Vleesschauwer *et al.*, 2012). Another study showed exogenous treatment of
331 rice leaves with brassinolide enhanced resistance to *Xoo* (Nakashita *et al.*, 2003). The
332 *Xanthomonas* effector Xoo2875 was shown to suppress immunity by interacting with OsBAK1, a
333 component of PTI and BR signalling (Yamaguchi *et al.*, 2013). In Arabidopsis, BRs were shown
334 to antagonize JA-mediated plant defense (Liao *et al.*, 2020). Strikingly, several components of BR
335 signalling were downregulated whereas JA signalling was positively regulated in BB42 (Tables
336 S6, S7, S8; Fig. 4A). Whether and how OsMAPK6-S84P affect BR homeostasis and its relation
337 with disease resistance warrants further investigations.

338 Our study leads to several questions such as: Is the novel MAPK6 variant constitutively
339 active? Does the variation affect the interactome of OsMAPK6? Are rice MAPK cascades guarded
340 by NLRs? Is rice NLR expression controlled by OsMAPK6-mediated signalling? How could
341 OsMAPK6 govern BR homeostasis, and what is the role of BR signalling in rice-*Xoo* interaction?
342 Do rice pathogens directly target the components of MAPK cascade to promote virulence? BB42
343 can also serve as a novel source of BB resistance as initial observations suggest that there is no
344 drastic effect on yield. However, further studies are needed to determine if BB42 has more subtle

345 reductions in yield as compared to the parental line. More research directed towards the above
346 questions would provide deeper insights into rice MAPK signalling, broaden our understanding of
347 plant immunity in crop species and also indicate whether BB42 can be a source of resistance that
348 can be used for rice improvement.

349 **EXPERIMENTAL PROCEDURES**

350 **Plant materials and bacterial strains**

351 Plant materials used for this study include the wildtype/parental cultivar Samba Mahsuri
352 (SM; BPT5204) and the EMS-induced mutant line named BB42. Nipponbare rice cultivar was
353 used as a susceptibility check for bacterial leaf streak disease scoring. *Xanthomonas oryzae* pv.
354 *oryzae* (*Xoo*) and *X. oryzae* pv. *oryzicola* (*Xoc*) isolates were cultured from the lab stocks and the
355 stocks obtained from Indian Institute of Rice Research, Hyderabad. The bacterial strains that were
356 used are listed in Table S1. The seeds were germinated on Petri plates at 28°C in darkness for 72
357 hours and under 12-hour photoperiod from days 4 to 7. Later the seedlings were potted onto soil
358 before transplanting to the field after 14-21 days of potting and grown in greenhouse conditions
359 under natural lighting.

360 **Plant inoculation**

361 Plants in the maximum tillering stage (50-60 days) were inoculated with *Xoo* isolates using
362 the clip inoculation method (Kauffman *et al.*, 1973). The *Xoo* isolates were grown in Peptone-
363 Sucrose (PS) broth (1% (w/v) peptone and 1% (w/v) sucrose) for 24 hours and the cells were
364 pelleted. The cells were further washed in sterile Milli-Q water one to two times and adjusted to
365 an optical density at 600nm (OD_{600}) of 1.0. Sterile scissors were used to dip into the bacterial
366 suspension and clip the fully expanded leaves ~3-4 cm from the leaf tip. The disease severity was
367 scored by measuring the lesion length from the site of inoculation after 14 days of inoculation. The
368 scoring was performed following the Rice Standard Evaluation System (IRRI, 2014). Inoculations
369 were done in green house with temperature maintained under 30°C for transcriptome analysis
370 studies and multiple-isolate screening. The parental lines and F_2 progenies were screened in the
371 rice field facility of CSIR-CCMB (17.41° N, 78.55° E) during Kharif 2020 with the *Xoo* strain
372 IXO1221. *Xoc* inoculation was performed in greenhouse conditions on 2-3 weeks old seedlings
373 through syringe infiltration of *Xoc* suspension at OD_{600} = 1.0. Lesion lengths were measured at 5
374 days post inoculation.

375 **Generation of mapping populations**

376 Two mapping populations were generated in this study. The populations were obtained by
377 using SM as recipient and BB42 as donor (SM x BB42) and vice versa (BB42 x SM). The F_1
378 plants, so generated, were tested for hybridity by Sanger sequencing of known SNPs between SM
379 and BB42, which were identified using whole genome sequencing data. The confirmed F_1 plants
380 were let to self-fertilize to obtain two independent segregating populations. F_2 populations with
381 244 progenies per population were screened for BB resistance as described above.

382 **Bulk sequencing and analysis**

383 F_2 plants from both the populations showing the extreme phenotypes i.e., resistance and
384 susceptibility to BB infection were selected to constitute the resistant and susceptible bulks,
385 respectively. An equal amount of leaves (15mg per leaf) were pooled from F_2 plants showing
386 identical phenotype for DNA isolation. DNA from the bulked leaves as well as the parental leaves
387 were isolated using the CTAB method and quantified using Qubit™ High-Sensitivity dsDNA
388 Assay in a Qubit™ 4 fluorometer (Thermo Fisher Scientific, USA). The quality of the DNA was
389 assessed on 0.8% agarose gel through electrophoresis. An amount of 1µg DNA from all the
390 samples was used to prepare sequencing libraries with TruSeq Nano DNA HT Sample Preparation
391 Kit (Illumina, USA) and qualified libraries were sequenced on Illumina NovaSeq 6000 platform
392 to obtain 2x150 bp reads at approximately 40X coverage. The library preparation and sequencing
393 were performed at the NGS facility of CSIR-CCMB. The sequenced reads were quality-checked
394 using *FastQC* and were provided as input for QTLseq pipeline (Sugihara *et al.*, 2020) to identify
395 the causal loci. SM reference genome (assembled in-house) was used for the gene mapping
396 analysis (Rao *et al.*, *in preparation*). *AUGUSTUS* in the *Galaxy* platform was used for annotating
397 the interval of interest (Afgan *et al.*, 2018; Stanke *et al.*, 2004). *SnpEff* was used for annotating the
398 variants (Cingolani *et al.*, 2012).

399 **Development of SNP markers and linkage analysis**

400 Two derived Cleaved Amplification Polymorphic Site (dCAPS) markers were developed
401 to distinguish the *OsMAPK6* alleles of SM and BB42. One marker was developed by introducing
402 a SacI restriction site in the SM allele while the other marker was developed by introducing a SmaI
403 restriction site in the BB42 allele. The primer sequences were designed based on the SM reference
404 sequence using dCAPS Finder 2.0 (Neff *et al.*, 2002). All the reactions were performed using 2X

405 KAPA Taq ReadyMix (Roche, Switzerland) with 500-1000 pmoles/µl primers and 20-40ng of the
406 template. The reaction conditions are as follows: 95°C for 5 minutes, 35 cycles of 95°C for 30
407 seconds, 58°C for 30 seconds and 72°C for 30 seconds, and 72°C for 5 minutes. The PCR samples
408 were then added with 0.5-1µl of corresponding restriction enzymes and incubated at 37°C for 6
409 hours to overnight before resolving them on a 2.5% agarose gel for 1 hour at 100V. Gel images
410 were captured on a gel documentation system (AlphaInnotech, USA). Further, another marker was
411 developed based on the tetra-primer amplification refractory mutation system (tetra-ARMS) PCR
412 (Ye *et al.*, 2001). A typical tetra-ARMS-PCR reaction contains four primers among which each of
413 the two inner primers is specific to the two alleles of interest. The tetra-ARMS reaction to
414 distinguish the *OsMAPK6* alleles was standardized, and the reaction composition is as follows:
415 500 nM of each primer, PCR buffer – 10mM tris-HCl (pH8.3), 20mM ammonium sulphate, 2mM
416 magnesium chloride, and 0.25mM of each dNTP, 0.2µl of 5U/µl Taq DNA polymerase (G-
417 biosciences), and 40ng of the template. The reaction conditions are as follows: 95°C for 5 minutes,
418 35 cycles of 95°C for 30 seconds, 58°C for 20 seconds and 72°C for 30 seconds, and 72°C for 5
419 minutes. The samples were resolved on a 2.5% agarose gel for one hour at 100V. To test the
420 linkage between the OsMAPK6 allele and BB resistance, we tested the genotype of seven resistant
421 progenies and seven susceptible progenies from the F_2 generation using the dCAPS marker that
422 was developed as mentioned above.

423 **Protein sequence analysis**

424 Homologous sequences of OsMAPK6 were retrieved from NCBI through a BLASTp
425 search. Sequences of all the rice MAPKs were obtained from RGAP database (Hamilton *et al.*,
426 2025). Multiple sequence alignment (MSA) was performed using Multalin (Corpet, 1988). ESPript
427 3 was used to visualize MSA results (Robert and Gouet, 2014). WebLogo was used to generate
428 sequence alignment logos (https://weblogo.berkeley.edu/logo.cgi) (Crooks *et al.*, 2004). One-click
429 mode of Phylogeny.fr server was used for constructing the maximum likelihood trees of MAPK6
430 homologues and the rice MAPKs (Dereeper *et al.*, 2008). Phylogenetic trees were annotated using
431 iTOL (http://itol.embl.de/) (Letunic and Bork, 2021).

432 **RNA sequencing and analysis**

433 SM and BB42 plants were inoculated with the *Xoo* isolate IXO1221 during the maximum
434 tillering stage. One-centimeter-long leaf samples from the site of clipping were collected at the

435 time of infection as control (0 hour/Mock) and 24-hour post infection (Xoo) from both SM and
436 BB42. The samples were collected from three independent plants serving as biological replicates.
437 The samples were flash-frozen immediately after collection and stored at -80°C until further
438 processing. RNA was isolated from the samples using RNeasy Plant RNA Isolation Kit (Qiagen,
439 Germany) with on-column DNA digestion using RNase-Free DNase Set (Qiagen, Germany).
440 Purified RNA was quantified using Qubit^{TM} RNA HS Assay Kit (Thermo Fisher Scientific, USA).
441 RNA integrity was assessed using agarose gel electrophoresis and BioAnalyzer 2100 (Agilent
442 Technologies, USA). 1 µg of intact total RNA samples were used for library preparation using
443 Illumina TruSeq Stranded Total RNA with Ribo-Zero Plant (Illumina, USA). Sequencing was
444 performed on Illumina's NovaSeq6000 platform with cycling conditions to obtain 2x100bp reads
445 on an S2 flow cell.

446 The raw data were obtained, and the quality was assessed using *FastQC*. Adapters and
447 low-quality reads were trimmed using *Trim Galore! RNA-STAR* was used to align the trimmed
448 reads to the rice genome (MSU Rice Genome Annotation Project - version 7). Reads that mapped
449 to the genes were quantified using *featureCounts*. Differential gene expression was obtained using
450 the R library *DEseq2.* Genes with a false discovery rate ≤ 0.05 and $\log_2$ fold change ≤ -1 or ≥ 1
451 were considered differentially expressed genes (DEGs). For gene ontology, and pathway analyses
452 ShinyGO was used. iDEP.96 was used for *k*-means clustering and further analysis (Ge *et al.*, 2018).
453 *Venny* was used for generating Venn diagrams (Oliveros, J.C., 2007). Protein domain enrichment
454 among the DEGs was performed in STRING v12.0 (Szklarczyk *et al.*, 2023). RNA sequence
455 statistics are provided in Table S3.

456 **Quantitative PCR for defense marker genes**

457 Complementary DNA (cDNA) was synthesized from 1-5 microgram RNA using EcoDry
458 cDNA Synthesis Kit (Takara) containing Oligo(dT). The reaction condition is as follows: 42°C for
459 60 minutes; 70°C for 10 minutes. The synthesized cDNA samples were diluted to 15-25ng/µl for
460 quantitative PCR (qPCR). qPCR was performed using PowerSYBR kit (Invitrogen) in triplicates
461 per primer-sample combination. The reaction composition is as follows: 5µl of 2X master mix,
462 0.5µl each of forward primer (5µM) and reverse primer (5µM), 1µl template, 3µl nuclease-free
463 water. The reactions were performed in 384-well plates at the following conditions: 50°C for 2
464 minutes, 95°C for 10minutes, 35 cycles of 95°C for 10 seconds and 60°C for 30seconds and melt

465 curve analysis between 60°C and 95°C. The reactions were set in Viaa7 (Applied Biosystems) or
466 CFX384 (BioRad) instruments. The primers for qPCR reactions were designed using QuantPrime
467 (Arvidsson *et al.*, 2008). The list of primers and corresponding sequences are provided in Table
468 S2.

469 **Immunoblotting**

470 For MAPK activation assay, one-week old SM and BB42 roots were treated with mock or 1µM
471 flg22 for 15 minutes. For assay in seedlings, 1-week laboratory-grown seedlings were harvested
472 and processed further. Protein samples were isolated from the above samples, resolved on a 12%
473 polyacrylamide SDS gel, transferred onto PVDF membrane and probed using the anti-Phospho-
474 erk1/2 antibody (#9101; 1:2000 dilution; Cell Signaling Technologies). The blots were stained
475 with Ponceau-S-stained for loading control.

476 For qualitative assessment of total phosphorylated proteins, SM and BB42 leaf samples from
477 plants in maximum tillering stage (~60 days) were processed as mentioned above and probed using
478 anti-Phosphoserine (ab9332; 1:1000; Abcam) and anti-Phosphothreonine/tyrosine (#9381; 1:3000;
479 Cell Signaling Technologies) antibodies. Ponceau-S-stained blot is used as loading control blots.
480 The immuno signals were visualized using HRP-conjugated anti-rabbit secondary antibody
481 (ab98440; 1:20000; Abcam) and ECL Western high-sensitivity substrate (Thermo Fisher
482 Scientific, USA).

483 **BR sensitivity assays**

484 All the assays pertinent to brassinosteroid treatment were performed as described earlier (Liu *et*
485 *al.*, 2015). Briefly, for coleoptile elongation assay, seeds of SM and BB42 were soaked overnight
486 in fresh water, washed and plated on Petri plates containing solvent control or 5µM 24-
487 epibrassinolide (Real-Gene Labs, UP, India) and grown further. The hypocotyl length was
488 measured one-week post germination in dark conditions. Grain parameters like length and width
489 were measured using a graduated ruler.

490 **Metabolite profiling**

491 Metabolite profiling and analysis was performed on field-grown SM and BB42 leaves during
492 maximum tillering stage essentially by following the steps as mentioned elsewhere (Gokulan *et*

493 *al.*, 2024). Sample preparation and processing were outsourced to Novelgene Technologies Pvt.
494 Ltd., Hyderabad, India.

495 **Statistical analyses**

496 The relevant statistical tests and considerations are provided in appropriate figure legends. Box
497 plots, bar plots, and multivariate dot plots were plotted on R4.2.2 using *ggplot* package and the
498 statistical parameters were integrated to the plots using the *ggpubr* package.

499

500 **Author contributions**

501 RVS, MSM, and HKP: conceptualization; RVS, MSM, HKP, and GCG: methodology; GCG:
502 formal analysis; GCG, MJ, DR, NG, ARS, NS, and DN: investigation; RVS, HKP, ST, MSM,
503 RMS, KMB, and GSL: resources; GCG: data curation; GCG: writing - original draft; GCG, RVS,
504 HKP, MSM, KMB, and GSL: writing - review & editing; GCG: visualization; RVS, HKP, and
505 MSM: supervision; RVS, HKP, and MSM: funding acquisition.

506 **Acknowledgements**

507 We thank the CCMB NGS Facility for nucleic acid sequencing services. We thank the skilled
508 workers at ICAR-IIRR and CSIR-CCMB for their support in field activities and maintenance. We
509 thank Sebastien Santini (CNRS/AMU IGS UMR7256) and the PACA Bioinfo platform for the
510 availability and management of the phylogeny.fr website. GCG, MJ, DR, NG, ARS, NS, and DN
511 thank the Council of Scientific and Industrial Research for fellowship. GCG thanks the Department
512 of Biotechnology for the MK Bhan - Young Researcher Fellowship.

513 **Supplementary information**

514 Figure S1: SM and BB42 are equally susceptible to *Xoc.*
515 Figure S2: F_2 phenotyping and marker development.
516 Figure S3: Mutation in OsMPAK6 does not affect gene splicing.
517 Figure S4: PCA plot of gene expression.
518 Figure S5: Pathway enrichment analysis among DEGs.
519 Figure S6: Protein domain enrichment among DEGs.
520 Figure S7: BB42 shows signs of autoimmunity.
521 Figure S8: Metabolite analysis of SM and BB42.

522 Figure S9: Pathway enrichment analysis of differentially accumulated metabolites.

523 Figure S10: Phylogeny of MAPK6 homologues across different forms of life.

524 Figure S11: Phylogeny of seventeen OsMAPK proteins.

525

526 Table S1: List of strains.

527 Table S2: List of primers.

528 Table S3: RNA-seq read statistics.

529 Table S4: Phenotype segregation analysis.

530 Table S5: DEG statistics.

531 Table S6: Differential expression of defense related genes.

532 Table S7: Differential expression of JAZ-encoding genes.

533 Table S8: Differential expression of BR-related genes.

534

535 Data S1: List of DEGs in across different comparisons.

536 Data S2: List of differentially accumulated metabolites.

537 **Conflict of interest**

538 No conflict of interest declared.

539 **Data availability**

540 The DNA sequence data of the F_2 bulks are deposited in NCBI SRA under the BioProject ID
541 PRJNA1235664. The RNA-seq data are submitted in NCBI Gene Expression Omnibus under the
542 accession GSE291968. The DNA sequence data of parental lines are reported in (Potupureddi *et*
543 *al.*, 2021). Any other materials and data are available upon reasonable request.

544 **Funding Statement**

545 This work was supported by Council of Scientific and Industrial Research's grant [MLP0121-
546 Phase I and Phase II] and the Scientific and Engineering Research Board's JC Bose fellowship to
547 RVS [SB/S2/JCB-12/2014].

548

549 **REFERENCES**

550 Abe, A., Kosugi, S., Yoshida, Kentaro, Natsume, S., Takagi, H., Kanzaki, H., et al. (2012) *Genome*
551 *sequencing reveals agronomically important loci in rice using MutMap*. *Nature*
552 *Biotechnology*, **30**, 174–178.
553 Afgan, E., Baker, D., Batut, B., Van Den Beek, M., Bouvier, D., Ech, M., et al. (2018) *The Galaxy*
554 *platform for accessible, reproducible and collaborative biomedical analyses: 2018 update*.
555 *Nucleic Acids Research*, **46**, W537–W544.
556 Albrecht, C., Boutrot, F., Segonzac, C., Schwessinger, B., Gimenez-Ibanez, S., Chinchilla, D., et
557 al. (2012) *Brassinosteroids inhibit pathogen-associated molecular pattern-triggered*
558 *immune signaling independent of the receptor kinase BAK1*. *Proc Natl Acad Sci U S A*,
559 **109**, 303–308.
560 Arvidsson, S., Kwasniewski, M., Riaño-Pachón, D.M., and Mueller-Roeber, B. (2008)
561 *QuantPrime - A flexible tool for reliable high-throughput primer design for quantitative*
562 *PCR*. *BMC Bioinformatics*, **9**, 1–15.
563 Belkhadir, Y., Jaillais, Y., Epple, P., Balsemão-Pires, E., Dangl, J.L., and Chory, J. (2012)
564 *Brassinosteroids modulate the efficiency of plant immune responses to microbe-associated*
565 *molecular patterns*. *Proc Natl Acad Sci U S A*, **109**, 297–302.
566 Berriri, S., Garcia, A.V., Frei dit Frey, N., Rozhon, W., Pateyron, S., Leonhardt, N., et al. (2012)
567 *Constitutively active mitogen-activated protein kinase versions reveal functions of*
568 *Arabidopsis MPK4 in pathogen defense signaling*. *Plant Cell*, **24**, 4281–4293.
569 Carpenter, S.C.D., Mishra, P., Ghoshal, C., Dash, P.K., Wang, L., Midha, S., et al. (2020) *An xa5*
570 *Resistance Gene-Breaking Indian Strain of the Rice Bacterial Blight Pathogen*
571 *Xanthomonas oryzae pv. oryzae Is Nearly Identical to a Thai Strain*. *Frontiers in*
572 *Microbiology*, **11**, 2328.
573 Chen, J., Wang, L., Yang, Z., Liu, H., Chu, C., Zhang, Z., et al. (2021) *The rice Raf-like MAPKKK*
574 *OsILA1 confers broad-spectrum resistance to bacterial blight by suppressing the*
575 *OsMAPKK4–OsMAPK6 cascade*. *Journal of Integrative Plant Biology*, **63**, 1815–1842.
576 Chen, X. and Ronald, P.C. (2011) *Innate immunity in rice*. *Trends in Plant Science*, **16**, 451–459.
577 Chujo, T., Miyamoto, K., Ogawa, S., Masuda, Y., Shimizu, T., Kishi-Kaboshi, M., et al. (2014)
578 *Overexpression of phosphomimic mutated OsWRKY53 leads to enhanced blast resistance*
579 *in rice*. *PLoS One*, **9**, e98737.
580 Cingolani, P., Platts, A., Wang, L.L., Coon, M., Nguyen, T., Wang, L., et al. (2012) *A program*
581 *for annotating and predicting the effects of single nucleotide polymorphisms, SnpEff: SNPs*
582 *in the genome of Drosophila melanogaster strain w1118; iso-2; iso-3*. *Fly*, **6**, 80–92.
583 Corpet, F. (1988) *Multiple sequence alignment with hierarchical clustering*. *Nucleic acids*
584 *research*, **16**, 10881–10890.
585 Crooks, G.E., Hon, G., Chandonia, J.-M., and Brenner, S.E. (2004) *WebLogo: a sequence logo*
586 *generator*. *Genome Res*, **14**, 1188–1190.
587 D Couto, C.Z. (2016) *Regulation of pattern recognition receptor signalling in plants*. *Nat. Rev.*
588 *Immunol.*, **16**, 537–552.
589 Dasari, A., Vemulapalli, P., Gonuguntla, R., Thota, D.K., Elumalai, P., Muppavarapu, K., et al.
590 (2022) *Improvement of bacterial blight resistance of the popular variety, Nellore Mahsuri*
591 *(NLR34449) through marker-assisted breeding*. *J Genet*, **101**, 7.
592 De Vleesschauwer, D., Van Buyten, E., Satoh, K., Balidion, J., Mauleon, R., Choi, I.-R., et al.
593 (2012) *Brassinosteroids Antagonize Gibberellin- and Salicylate-Mediated Root Immunity*
594 *in Rice*. *Plant Physiology*, **158**, 1833–1846.

595 Dereeper, A., Guignon, V., Blanc, G., Audic, S., Buffet, S., Chevenet, F., et al. (2008)
596 *Phylogeny.fr: robust phylogenetic analysis for the non-specialist*. *Nucleic Acids Res*, **36**,
597 W465-469.
598 Fiyaz, R.A., Shivani, D., Chaithanya, K., Mounika, K., Chiranjeevi, M., Laha, G.S., et al. (2022)
599 *Genetic Improvement of Rice for Bacterial Blight Resistance: Present Status and Future*
600 *Prospects*. *Rice Science*, **29**, 118–132.
601 Freh, M., Gao, J., Petersen, M., and Panstruga, R. (2022) *Plant autoimmunity—fresh insights into*
602 *an old phenomenon*. *Plant Physiology*, **188**, 1419–1434.
603 Gao, M., Liu, J., Bi, D., Zhang, Z., Cheng, F., Chen, S., and Zhang, Y. (2008) *MEKK1,*
604 *MKK1/MKK2 and MPK4 function together in a mitogen-activated protein kinase cascade*
605 *to regulate innate immunity in plants*. *Cell Res*, **18**, 1190–1198.
606 Ge, S.X., Son, E.W., and Yao, R. (2018) *iDEP: an integrated web application for differential*
607 *expression and pathway analysis of RNA-Seq data*. *BMC Bioinformatics*, **19**, 534.
608 Genot, B., Lang, J., Berriri, S., Garmier, M., Gilard, F., Pateyron, S., et al. (2017) *Constitutively*
609 *Active Arabidopsis MAP Kinase 3 Triggers Defense Responses Involving Salicylic Acid*
610 *and SUMM2 Resistance Protein*. *Plant Physiology*, **174**, 1238–1249.
611 Gokulan, C.G., Bangale, U., Balija, V., Ballichatla, S., Potupureddi, G., Rao, D., et al. (2024)
612 *Multiomics-assisted characterization of rice-Yellow Stem Borer interaction provides*
613 *genomic and mechanistic insights into stem borer resistance in rice*. *Theor Appl Genet*,
614 **137**, 122.
615 Goto, M. (1992) *Fundamentals of bacterial plant pathology*, 1st edn. Academic Press.
616 Greene, E.A., Codomo, C.A., Taylor, N.E., Henikoff, J.G., Till, B.J., Reynolds, S.H., et al. (2003)
617 *Spectrum of Chemically Induced Mutations From a Large-Scale Reverse-Genetic Screen*
618 *in Arabidopsis*. *Genetics*, **164**, 731–740.
619 Hamilton, J.P., Li, C., and Buell, C.R. (2025) *The rice genome annotation project: an updated*
620 *database for mining the rice genome*. *Nucleic Acids Research*, **53**, D1614–D1622.
621 Heese, A., Hann, D.R., Gimenez-Ibanez, S., Jones, A.M.E., He, K., Li, J., et al. (2007) *The*
622 *receptor-like kinase SERK3/BAK1 is a central regulator of innate immunity in plants*. *Proc.*
623 *Natl. Acad. Sci. U.S.A.*, **104**, 12217–12222.
624 Hilaire, E., Young, S.A., Willard, L.H., McGee, J.D., Sweat, T., Chittoor, J.M., et al. (2007)
625 *Vascular Defense Responses in Rice: Peroxidase Accumulation in Xylem Parenchyma*
626 *Cells and Xylem Wall Thickening*. *https://doi.org/10.1094/MPMI.2001.14.12.1411*, **14**,
627 1411–1419.
628 Huang, N., Angeles, E.R., Domingo, J., Magpantay, G., Singh, S., Zhang, G., et al. (1997)
629 *Pyramiding of bacterial blight resistance genes in rice: marker-assisted selection using*
630 *RFLP and PCR*. *Theoretical and Applied Genetics 1997 95:3*, **95**, 313–320.
631 IRRI (2014) *Standard evaluation system for rice. International Rice Research Institute*. IRRI.
632 Jamaloddin, M., Mahender, A., Gokulan, C.G., Balachiranjeevi, C., Maliha, A., Patel, H.K., and
633 Ali, J. (2021) *Molecular Approaches for Disease Resistance in Rice*. In: *Rice Improvement*
634 , pp. 315–378. Cham: Springer International Publishing.
635 Jamaloddin, Md., Durga Rani, Ch.V., Swathi, G., Anuradha, Ch., Vanisri, S., Rajan, C.P.D., et al.
636 (2020) *Marker Assisted Gene Pyramiding (MAGP) for bacterial blight and blast resistance*
637 *into mega rice variety "Tellahamsa." PLOS ONE*, **15**, e0234088.
638 Jhingan, S., Kumar, A., Harloff, H.-J., Dreyer, F., Abbadi, A., Beckmann, K., et al. (2023) *Direct*
639 *access to millions of mutations by whole genome sequencing of an oilseed rape mutant*
640 *population*. *The Plant Journal*, **113**, 866–880.

641 Jiang, N., Yan, J., Liang, Y., Shi, Y., He, Z., Wu, Y., et al. (2020) *Resistance Genes and their*
642 *Interactions with Bacterial Blight/Leaf Streak Pathogens (Xanthomonas oryzae) in Rice*
643 *(Oryza sativa L.)—an Updated Review*. *Rice*, **13**, 1–12.
644 Jiang, R., Zhou, S., Da, X., Yan, P., Wang, K., Xu, J., and Mo, X. (2023) *OsMKK6 Regulates*
645 *Disease Resistance in Rice*. *International Journal of Molecular Sciences*, **24**, 12678.
646 Jones, J.D.G. and Dangl, J.L. (2006) *The plant immune system*. *Nature 2006 444:7117*, **444**, 323–
647 329.
648 Jones, J.D.G., Vance, R.E., and Dangl, J.L. (2016) *Intracellular innate immune surveillance*
649 *devices in plants and animals*. *Science*, **354**.
650 Joshi, J.B., Arul, L., Ramalingam, J., and Uthandi, S. (2020) *Review Advances in the Xoo-rice*
651 *pathosystem interaction and its exploitation in disease management*. *Journal of*
652 *Biosciences*, **45**.
653 K. Reddy, A.P. (1979) *Relationship of Bacterial Leaf Blight Severity to Grain Yield of Rice*.
654 *Phytopathology*, **69**, 967.
655 Kauffman, H.E., Reddy, A.P.K., Hsieh, S.P.Y., and Merca, S.D. (1973) *An improved technique*
656 *for evaluating resistance of rice varieties to Xanthomonas oryzae. Plant Dis. Rep*, **57**, 737–
657 741.
658 Kaur, A., Bansal, K., and Patil, P.B. (2020) *Extensive Genomic Rearrangements along with*
659 *Distinct Mobilome and TALome are Associated with Extreme Pathotypes of a Rice*
660 *Pathogen*. *Genome Biology and Evolution*, **12**, 3951–3956.
661 Kim, S.-H., Oikawa, T., Kyozuka, J., Wong, H.L., Umemura, K., Kishi-Kaboshi, M., et al. (2012)
662 *The bHLH Rac Immunity1 (RAI1) Is Activated by OsRac1 via OsMAPK3 and OsMAPK6*
663 *in Rice Immunity*. *Plant Cell Physiol*, **53**, 740–754.
664 Kishi-Kaboshi, M., Okada, K., Kurimoto, L., Murakami, S., Umezawa, T., Shibuya, N., et al.
665 (2010) *A rice fungal MAMP-responsive MAPK cascade regulates metabolic flow to*
666 *antimicrobial metabolite synthesis*. *Plant J*, **63**, 599–612.
667 Lang, J., Genot, B., Bigeard, J., and Colcombet, J. (2022) *MPK3 and MPK6 control salicylic acid*
668 *signaling by up-regulating NLR receptors during pattern- and effector-triggered immunity*.
669 *Journal of Experimental Botany*, **73**, 2190–2205.
670 Lang, J., Genot, B., Hirt, H., and Colcombet, J. (2017) *Constitutive activity of the Arabidopsis*
671 *MAP Kinase 3 confers resistance to Pseudomonas syringae and drives robust immune*
672 *responses*. *Plant Signaling & Behavior*, **12**, e1356533.
673 Letunic, I. and Bork, P. (2021) *Interactive Tree Of Life (iTOL) v5: an online tool for phylogenetic*
674 *tree display and annotation*. *Nucleic Acids Research*, **49**, W293–W296.
675 Lian, K., Gao, F., Sun, T., van Wersch, R., Ao, K., Kong, Q., et al. (2018) *MKK6 Functions in*
676 *Two Parallel MAP Kinase Cascades in Immune Signaling*. *Plant Physiol*, **178**, 1284–1295.
677 Liao, K., Peng, Y.-J., Yuan, L.-B., Dai, Y.-S., Chen, Q.-F., Yu, L.-J., et al. (2020) *Brassinosteroids*
678 *Antagonize Jasmonate-Activated Plant Defense Responses through BRI1-EMS-*
679 *SUPPRESSOR1 (BES1)1*. *Plant Physiol*, **182**, 1066–1082.
680 Lieberherr, D., Thao, N.P., Nakashima, A., Umemura, K., Kawasaki, T., and Shimamoto, K.
681 (2005) *A sphingolipid elicitor-inducible mitogen-activated protein kinase is regulated by*
682 *the small GTPase OsRac1 and heterotrimeric G-protein in rice 1[w]*. *Plant Physiol*, **138**,
683 1644–1652.
684 Liu, S., Hua, L., Dong, S., Chen, H., Zhu, X., Jiang, J., et al. (2015) *OsMAPK6, a mitogen-*
685 *activated protein kinase, influences rice grain size and biomass production*. *Plant Journal*,
686 **84**, 672–681.

687 Loveless, A. (1969) *Possible relevance of O-6 alkylation of deoxyguanosine to the mutagenicity*
688 *and carcinogenicity of nitrosamines and nitrosamides*. *Nature*, **223**, 206–207.
689 Ma, Z., Qin, G., Zhang, Y., Liu, C., Wei, M., Cen, Z., et al. (2021) *Bacterial leaf streak 1 encoding*
690 *a mitogen-activated protein kinase confers resistance to bacterial leaf streak in rice*. *The*
691 *Plant Journal*, **107**, 1084–1101.
692 Meng, X. and Zhang, S. (2013) *MAPK Cascades in Plant Disease Resistance Signaling*. *Annu.*
693 *Rev. Phytopathol.*, **51**, 245–266.
694 Mew, T.W. (1993) *Focus on Bacterial Blight of Rice*. *Plant Disease*, **77**, 5.
695 Mishra, D., Vishnupriya, M.R., Anil, M.G., Konda, K., Raj, Y., and Sonti, R.V. (2013) *Pathotype*
696 *and Genetic Diversity amongst Indian Isolates of Xanthomonas oryzae pv. oryzae*. *PLOS*
697 *ONE*, **8**, e81996.
698 Nakashita, H., Yasuda, M., Nitta, T., Asami, T., Fujioka, S., Arai, Y., et al. (2003) *Brassinosteroid*
699 *functions in a broad range of disease resistance in tobacco and rice*. *The Plant Journal*,
700 **33**, 887–898.
701 Neff, M.M., Turk, E., and Kalishman, M. (2002) *Web-based primer design for single nucleotide*
702 *polymorphism analysis*. *Trends in genetics : TIG*, **18**, 613–615.
703 Niño-Liu, D.O., Ronald, P.C., and Bogdanove, A.J. (2006) *Xanthomonas oryzae pathovars: model*
704 *pathogens of a model crop*. *Molecular Plant Pathology*, **7**, 303–324.
705 Oliva, R., Ji, C., Atienza-Grande, G., Huguet-Tapia, J.C., Perez-Quintero, A., Li, T., et al. (2019)
706 *Broad-spectrum resistance to bacterial blight in rice using genome editing*. *Nature*
707 *Biotechnology*, **37**, 1344–1350.
708 Oliveros, J.C. (2007) *Venny. An interactive tool for comparing lists with Venn's diagrams.*
709 Ou, S.H. (1973) *A handbook of rice diseases in the tropics.* University of Illinois at Urbana-
710 Champaign: International Rice Research Institute.
711 Ou, S.H. (1985) *Rice diseases*, 2nd edn. Commonwealth Mycological Institute.
712 Pontiggia, D., Benedetti, M., Costantini, S., De Lorenzo, G., and Cervone, F. (2020) *Dampening*
713 *the DAMPs: How Plants Maintain the Homeostasis of Cell Wall Molecular Patterns and*
714 *Avoid Hyper-Immunity*. *Frontiers in Plant Science*, **0**, 2010.
715 Potupureddi, G., Balija, V., Ballichatla, S., Gokulan, C.G., Awalellu, K., Lekkala, S., et al. (2021)
716 *Mutation resource of Samba Mahsuri revealed the presence of high extent of variations*
717 *among key traits for rice improvement*. *PLOS ONE*, **16**, e0258816.
718 Pradhan, S.K., Nayak, D.K., Mohanty, S., Behera, L., Barik, S.R., Pandit, E., et al. (2015)
719 *Pyramiding of three bacterial blight resistance genes for broad-spectrum resistance in*
720 *deepwater rice variety, Jalmagna*. *Rice*, **8**, 19.
721 Quibod, I.L., Atieza-Grande, G., Oreiro, E.G., Palmos, D., Nguyen, M.H., Coronejo, S.T., et al.
722 (2020) *The Green Revolution shaped the population structure of the rice pathogen*
723 *Xanthomonas oryzae pv. oryzae*. *ISME J*, **14**, 492–505.
724 Robert, X. and Gouet, P. (2014) *Deciphering key features in protein structures with the new*
725 *ENDscript server*. *Nucleic Acids Research*, **42**.
726 Rodriguez, M.C.S., Petersen, M., and Mundy, J. (2010) *Mitogen-activated protein kinase*
727 *signaling in plants*. *Annu Rev Plant Biol*, **61**, 621–649.
728 Savary, S., Willocquet, L., Pethybridge, S.J., Esker, P., McRoberts, N., and Nelson, A. (2019) *The*
729 *global burden of pathogens and pests on major food crops*. *Nature Ecology and Evolution*,
730 **3**, 430–439.
731 Stanke, M., Steinkamp, R., Waack, S., and Morgenstern, B. (2004) *AUGUSTUS: a web server for*
732 *gene finding in eukaryotes*. *Nucleic Acids Research*, **32**, W309–W312.

733 Su, J., Yang, L., Zhu, Q., Wu, H., He, Y., Liu, Y., et al. (2018) *Active photosynthetic inhibition*
734 *mediated by MPK3/MPK6 is critical to effector-triggered immunity*. *PLOS Biology*, **16**,
735 e2004122.
736 Sugihara, Y., Young, L., Yaegashi, H., Natsume, S., Shea, D.J., Takagi, H., et al. (2020) *High-*
737 *performance pipeline for MutMap and QTL-seq*. *bioRxiv*.
738 Sun, T. and Zhang, Y. (2022) *MAP kinase cascades in plant development and immune signaling*.
739 *EMBO reports*, **23**, e53817.
740 Sundaram, R.M., Vishnupriya, M.R., Biradar, S.K., Laha, G.S., Reddy, G.A., Rani, N.S., et al.
741 (2008) *Marker assisted introgression of bacterial blight resistance in Samba Mahsuri, an*
742 *elite indica rice variety*. *Euphytica*, **160**, 411–422.
743 Szklarczyk, D., Kirsch, R., Koutrouli, M., Nastou, K., Mehryary, F., Hachilif, R., et al. (2023) *The*
744 *STRING database in 2023: protein-protein association networks and functional*
745 *enrichment analyses for any sequenced genome of interest*. *Nucleic Acids Res*, **51**, D638–
746 D646.
747 Takagi, H., Abe, A., Yoshida, K., Kosugi, S., Natsume, S., Mitsuoka, C., et al. (2013) *QTL-seq:*
748 *Rapid mapping of quantitative trait loci in rice by whole genome resequencing of DNA*
749 *from two bulked populations*. *Plant Journal*, **74**, 174–183.
750 Till, B.J., Cooper, J., Tai, T.H., Colowit, P., Greene, E.A., Henikoff, S., and Comai, L. (2007)
751 *Discovery of chemically induced mutations in rice by TILLING*. *BMC Plant Biology*, **7**, 1–
752 12.
753 Tsuda, K., Mine, A., Bethke, G., Igarashi, D., Botanga, C.J., Tsuda, Y., et al. (2013) *Dual*
754 *Regulation of Gene Expression Mediated by Extended MAPK Activation and Salicylic Acid*
755 *Contributes to Robust Innate Immunity in Arabidopsis thaliana*. *PLOS Genetics*, **9**,
756 e1004015.
757 Wang, D., Wang, H., Liu, Q., Tu, R., Zhou, X., Zhang, Y., et al. (2021) *Reduction of OsMPK6*
758 *activity by a R89K mutation induces cell death and bacterial blight resistance in rice*. *Plant*
759 *Cell Rep*, **40**, 835–850.
760 Xiaobo, Z., Mu, Z., Mawsheng, C., Xuewei, C., and Jing, W. (2020) *Deciphering Rice Lesion*
761 *Mimic Mutants to Understand Molecular Network Governing Plant Immunity and Growth*.
762 *Rice Science*, **27**, 278–288.
763 Xu, R., Duan, P., Yu, H., Zhou, Z., Zhang, B., Wang, R., et al. (2018) *Control of Grain Size and*
764 *Weight by the OsMKKK10-OsMKK4-OsMAPK6 Signaling Pathway in Rice*. *Molecular*
765 *Plant*, **11**, 860–873.
766 Yamaguchi, K., Nakamura, Y., Ishikawa, K., Yoshimura, Y., Tsuge, S., and Kawasaki, T. (2013)
767 *Suppression of rice immunity by Xanthomonas oryzae type III effector Xoo2875*. *Biosci*
768 *Biotechnol Biochem*, **77**, 796–801.
769 Ye, S., Dhillon, S., Ke, X., Collins, A.R., and Day, I.N.M. (2001) *An efficient procedure for*
770 *genotyping single nucleotide polymorphisms*. *Nucleic acids research*, **29**, 88–88.
771 Yi, J., Lee, Y.-S., Lee, D.-Y., Cho, M.-H., Jeon, J.-S., and An, G. (2016) *OsMPK6 plays a critical*
772 *role in cell differentiation during early embryogenesis in Oryza sativa*. *J Exp Bot*, **67**,
773 2425–2437.
774 Yuan, M., Jiang, Z., Bi, G., Nomura, K., Liu, M., Wang, Y., et al. (2021) *Pattern-recognition*
775 *receptors are required for NLR-mediated plant immunity*. *Nature*, **592**, 105–109.
776 Yugander, A., Ershad, M., Muthuraman, P.P., Prakasam, V., Ladhalakshmi, D., Sheshu Madhav,
777 M., et al. (2022) *Understanding the variability of rice bacterial blight pathogen,*

Xanthomonas oryzae pv. oryzae in Andhra Pradesh, India. *Journal of Basic Microbiology*, **62**, 185–196.

Yugander, A., Sundaram, R.M., Ladhalakshmi, D., Hajira, S.K., Prakasam, V., Prasad, M.S., et al. (2017) *Virulence profiling of Xanthomonas oryzae pv. oryzae isolates, causing bacterial blight of rice in India*. *European Journal of Plant Pathology*, **149**, 171–191.

Zhang, Z., Liu, Y., Huang, H., Gao, M., Wu, D., Kong, Q., and Zhang, Y. (2017) *The NLR protein SUMM2 senses the disruption of an immune signaling MAP kinase cascade via CRCK3*. *EMBO Rep*, **18**, 292–302.

Zhang, Z., Wu, Y., Gao, M., Zhang, J., Kong, Q., Liu, Y., et al. (2012) *Disruption of PAMP-Induced MAP Kinase Cascade by a Pseudomonas syringae Effector Activates Plant Immunity Mediated by the NB-LRR Protein SUMM2*. *Cell Host & Microbe*, **11**, 253–263.

Zhao, H., Li, J., Yang, L., Qin, G., Xia, C., Xu, X., et al. (2021) *An inferred functional impact map of genetic variants in rice*. *Molecular Plant*, **14**, 1584–1599.

Zipfel, C. and Felix, G. (2005) *Plants and animals: A different taste for microbes? Current Opinion in Plant Biology*, **8**, 353–360.

795 **Table 1:** List of high-frequency SNPs identified within the mapped genomic interval, their SNP
796 indices, and effect.

Chr	Pos[a]	SNP index (SM x BB42)	SNP index (BB42 x SM)	Effect
Chr6	2243785	0.76	0.72	Intron variant
Chr6	2358077	0.81	1.00	Intron variant
Chr6	2379923	0.84	0.94	Downstream gene variant
Chr6	**2664062**	**0.94**	**0.90**	**Missense variant & splice region variant;** SIFT - deleterious (0)
Chr6	3057969	0.88	0.81	Downstream gene variant

797 [a] Coordinates in SM reference genome

798

799 **Figure 1**: **BB42 is a dwarf and bacterial blight resistant derivative of SM.** (A) and (B)
800 Comparison of the morphological features of SM and BB42 showing a significantly reduced height
801 of the latter. The statistical significance was calculated using unpaired two-tailed Student's *t* test.
802 Number of samples: SM=15, BB42=13. (C) Representative leaves of SM and BB42 showing the
803 disease symptoms at 14 days post inoculation (dpi). (D) Lesion length readings of *Xoo* infected
804 SM and BB42 plants at 14 days post inoculation. Fully expanded leaves were clip inoculated with
805 *Xoo* suspension at OD_{600} 1.0 (n>5). Statistical significance was calculated using one-way Anova
806 and comparisons between groups were performed using Tukey's HSD (Honest Significant
807 Difference) test with a 95% family-wise confidence level. $P<0.05$ was considered statistically
808 significant. In (B) and (D) boxes represent the 25th to 75th percentile while the line within the box
809 indicates the median. The whiskers extend to maximum and minimum data points that are within
810 1.5 times the interquartile range. Red dots indicate outliers.

811

812 **Figure 2: A novel mutation in *OsMAPK6* is linked to BB resistance.** Allele frequency plots of
813 chromosome 6 indicating the mapped regions in two F_2 population: (A) SM x BB42 and (B) BB42
814 x SM. The top plot represents the regression analysis of SNP-index of resistant bulk, middle plot
815 represents that of susceptible bulk, and the bottom plot indicates the delta SNP-index plot. The red
816 line is the moving average line plotted by averaging the SNP or delta SNP indices in 2Mb windows
817 and a 100kb step size. Each dot represents an SNP. The transparent orange bar indicates the
818 mapped genomic interval. (C) Schematic gene diagram of *OsMAPK6* indicating the affected base
819 (red arrow) and the amino acid substitution caused. (D) Multiple sequence alignment logo of 100
820 plant homologues of MAPK6 spanning the Serine residue of interest (red arrowhead). (E)
821 Genotyping of selected F_2 progenies using MAPK6 allele-specific PCR markers showing co-
822 segregation of the mutant allele with resistance.

823

824 **Figure 3: SM and BB42 share a substantial *Xoo*-mediated transcriptional landscape.** (A)
825 Number of Differentially Expressed Genes (DEGs) identified in various comparisons of the
826 transcriptome data. (B) Venn diagram showing common and unique differential gene expression
827 patterns in SM and BB42 samples challenged with *Xoo*. Up and Down mean upregulation or
828 downregulation of genes in *Xoo* treated condition as compared to mock treated condition in the
829 mentioned genotypes. (C) k-means clustering of gene expression profiles of the top 2000 genes.
830 Lines with different colours indicate different clusters based on the gene expression values.
831 Number of genes within each cluster is provided in the legend. Enriched terms adjacent to each
832 cluster are the GO terms that are enriched within corresponding clusters.

833

834 **Figure 4: BB42 exhibits constitutive immunity.** (A) Gene ontology term enrichment of the genes
835 that are upregulated (top panel) or downregulated (bottom panel) in mock samples of BB42 as
836 compared to the corresponding SM samples. (B) Box plots showing the abundance of certain
837 primary and secondary metabolites that are differentially accumulated between SM and BB42. The
838 raw peak intensities were normalised and plotted on the y-axis. The numbers above the horizontal
839 lines indicate the *P*-values as calculated using unpaired Student's *t*-test considering equal variance
840 between samples. $P<0.05$ is considered statistically significant. Boxes represent the 25th to 75th
841 percentile while the line within the box indicates the median. The whiskers extend to maximum
842 and minimum data points.

843

844 **Figure 5: Brassinosteroid signalling is impaired in BB42.** (A) Comparison of grain size of SM
845 and BB42. Scale bar = 1 cm. (B) and (C) bar graphs depicting the grain length and grain width,
846 respectively, of SM and BB42. N=30. Bars are drawn to average and the error bars indicate
847 standard deviation. The dots represent the data points. (D) Box plots showing the length of the
848 hypocotyl upon treatment of the seeds with mock solution or solution containing 5μM 24-
849 epibrassinolide. Boxes represent the 25th to 75th percentile while the line within the box indicates
850 the median. The whiskers extend to maximum and minimum data points that are within 1.5 times
851 the interquartile range. Solid black dots outside the whiskers, if any, indicate outliers. N>10. The
852 numbers above the horizontal line indicates *P*-values as calculated using unpaired Student's *t*-test
853 considering equal sample variance. $P<0.05$ is considered statistically significant. (E) Box plot
854 showing the abundance of brassinolide in SM and BB42 leaves. Boxes represent the 25th to 75th
855 percentile while the line within the box indicates the median. The whiskers extend to maximum
856 and minimum data points.

Figures

Figure 1 to 5.

A novel allele of *Mitogen Activated Protein Kinase 6* is linked to disease resistance and constitutive immunity in rice.

Gokulan C.G.[1,6,†], Mohammed Jamaloddin[1,†], Deepti Rao[1], Namami Gaur[1,2], Amita Rani Supriyo[1], Nisha Sao[1], Deepak Niranjan[1,7], Shrish Tiwari[1], Gouri S. Laha[3], Kalyani M. Barbadikar[3], Raman Meenakshi Sundaram[3], Sheshu Madhav Maganti[3,4,*], Hitendra K. Patel[1,5,*], Ramesh V. Sonti[1,7,*]

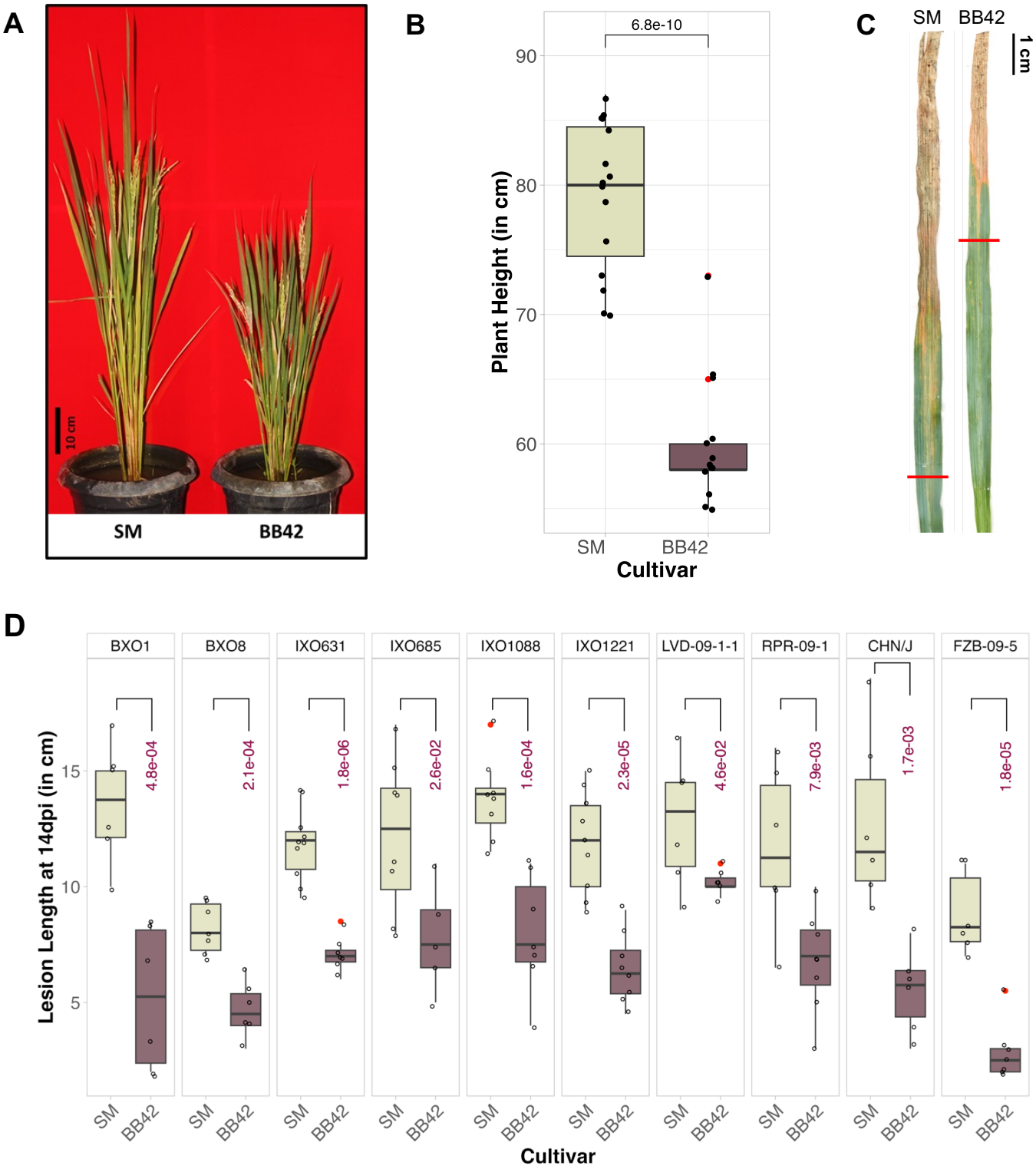
A
10 cm
SM
BB42
B
6.8e-10
Plant Height (in cm)
90
80
70
60
SM
BB42
Cultivar
C
SM
BB42
1 cm
D
BXO1
BXO8
IXO631
IXO685
IXO1088
IXO1221
LVD-09-1-1
RPR-09-1
CHN/J
FZB-09-5
4.8e-04
2.1e-04
1.8e-06
2.6e-02
1.6e-04
2.3e-05
4.6e-02
7.9e-03
1.7e-03
1.8e-05
Lesion Length at 14dpi (in cm)
15
10
5
SM
BB42
Cultivar

Figure 1: **BB42 is a dwarf and bacterial blight resistant derivative of Samba Mahsuri (SM).** (A) and (B) Comparison of the morphological features of SM and BB42 showing a significantly reduced height of the latter. The statistical significance was calculated using unpaired two-tailed Student's *t* test. Number of samples: SM=15, BB42=13. (C) Representative leaves of SM and BB42 showing the disease symptoms at 14 days post inoculation (dpi). (D) Lesion length readings of *Xoo* infected SM and BB42 plants at 14 days post inoculation. Fully expanded leaves were clip inoculated with *Xoo* suspension at OD_{600} 1.0 (n>5). Statistical significance was calculated using one-way Anova and comparisons between groups were performed using Tukey's HSD (Honest Significant Difference) test with a 95% family-wise confidence level. $P<0.05$ was considered statistically significant. In (B) and (D) boxes represent the 25th to 75th percentile while the line within the box indicates the median. The whiskers extend to maximum and minimum data points that are within 1.5 times the interquartile range. Red dots indicate outliers.

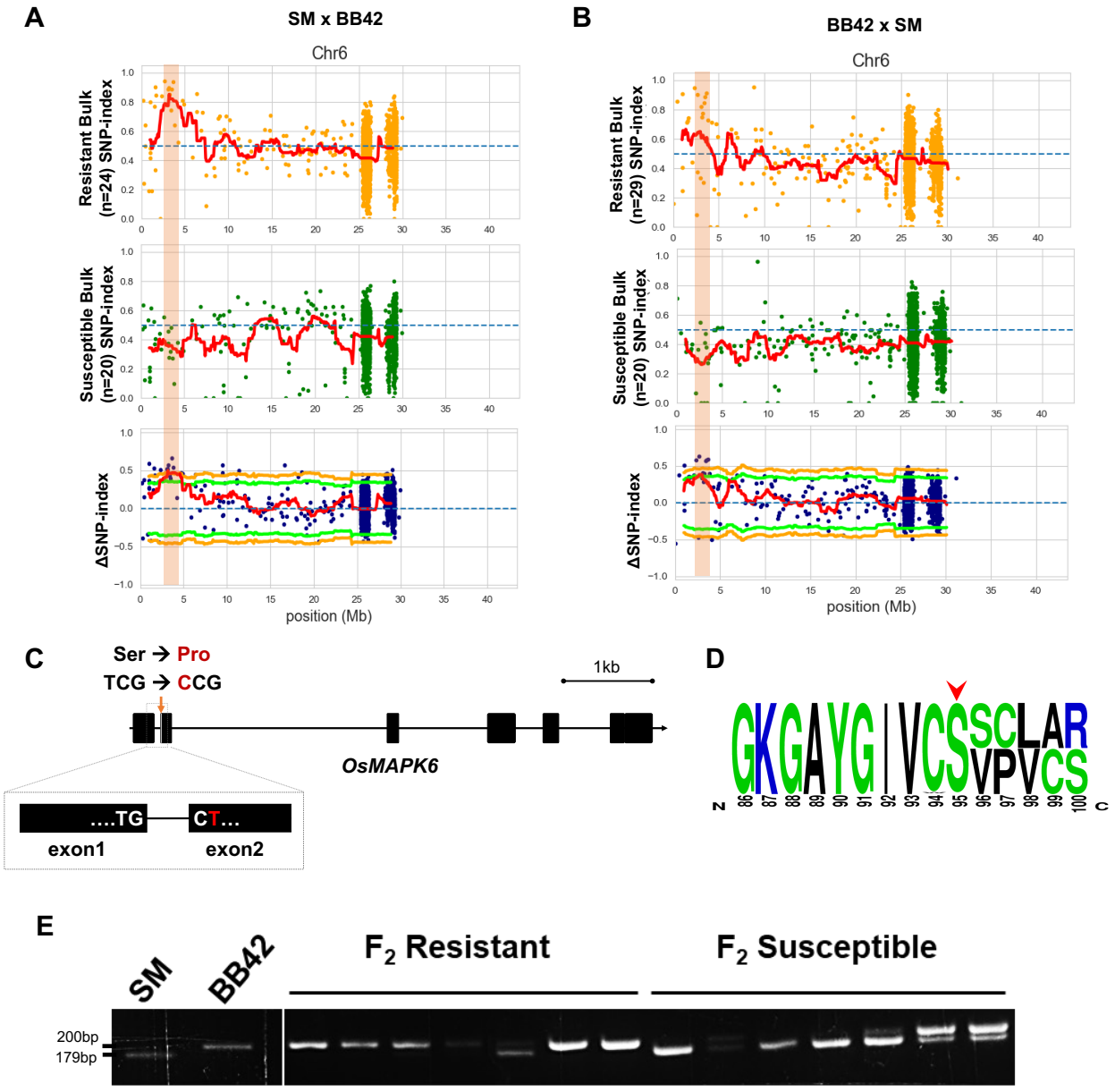

Figure 2: A novel mutation in *OsMAPK6* is linked to BB resistance. Allele frequency plots of chromosome 6 indicating the mapped regions in two F_2 population: (A) SM x BB42 and (B) BB42 x SM. The top plot represents the regression analysis of SNP-index of resistant bulk, middle plot represents that of susceptible bulk, and the bottom plot indicates the delta SNP-index plot. The red line is the moving average line plotted by averaging the SNP or delta SNP indices in 2Mb windows and a 100kb step size. Each dot represents an SNP. The transparent orange bar indicates the mapped genomic interval. (C) Schematic gene diagram of *OsMAPK6* indicating the affected base (red arrow) and the amino acid substitution caused. (D) Multiple sequence alignment logo of 100 plant homologues of MAPK6 spanning the Serine residue of interest (red arrowhead). (E)

Genotyping of selected F_2 progenies using MAPK6 allele-specific PCR markers showing co-segregation of the mutant allele with resistance.

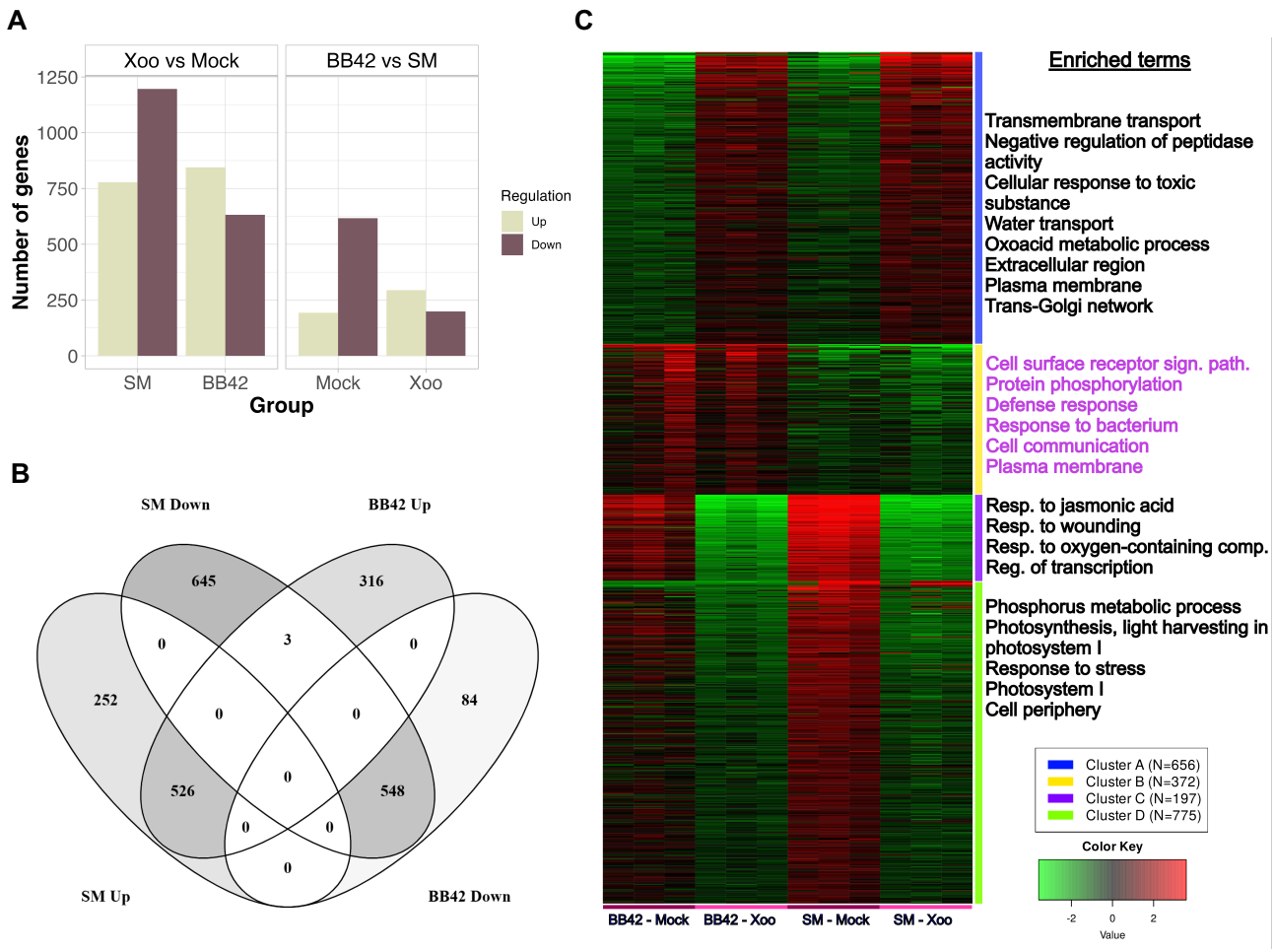

Figure 3: SM and BB42 share a substantial *Xoo*-mediated transcriptional landscape. (A) Number of Differentially Expressed Genes (DEGs) identified in various comparisons of the transcriptome data. (B) Venn diagram showing common and unique differential gene expression patterns in SM and BB42 samples challenged with *Xoo*. Up and Down mean upregulation or downregulation of genes in *Xoo* treated condition as compared to mock treated condition in the mentioned genotypes. (C) k-means clustering of gene expression profiles of the top 2000 genes. Lines with different colours indicate different clusters based on the gene expression values. Number of genes within each cluster is provided in the legend. Enriched terms adjacent to each cluster are the GO terms that are enriched within corresponding clusters.

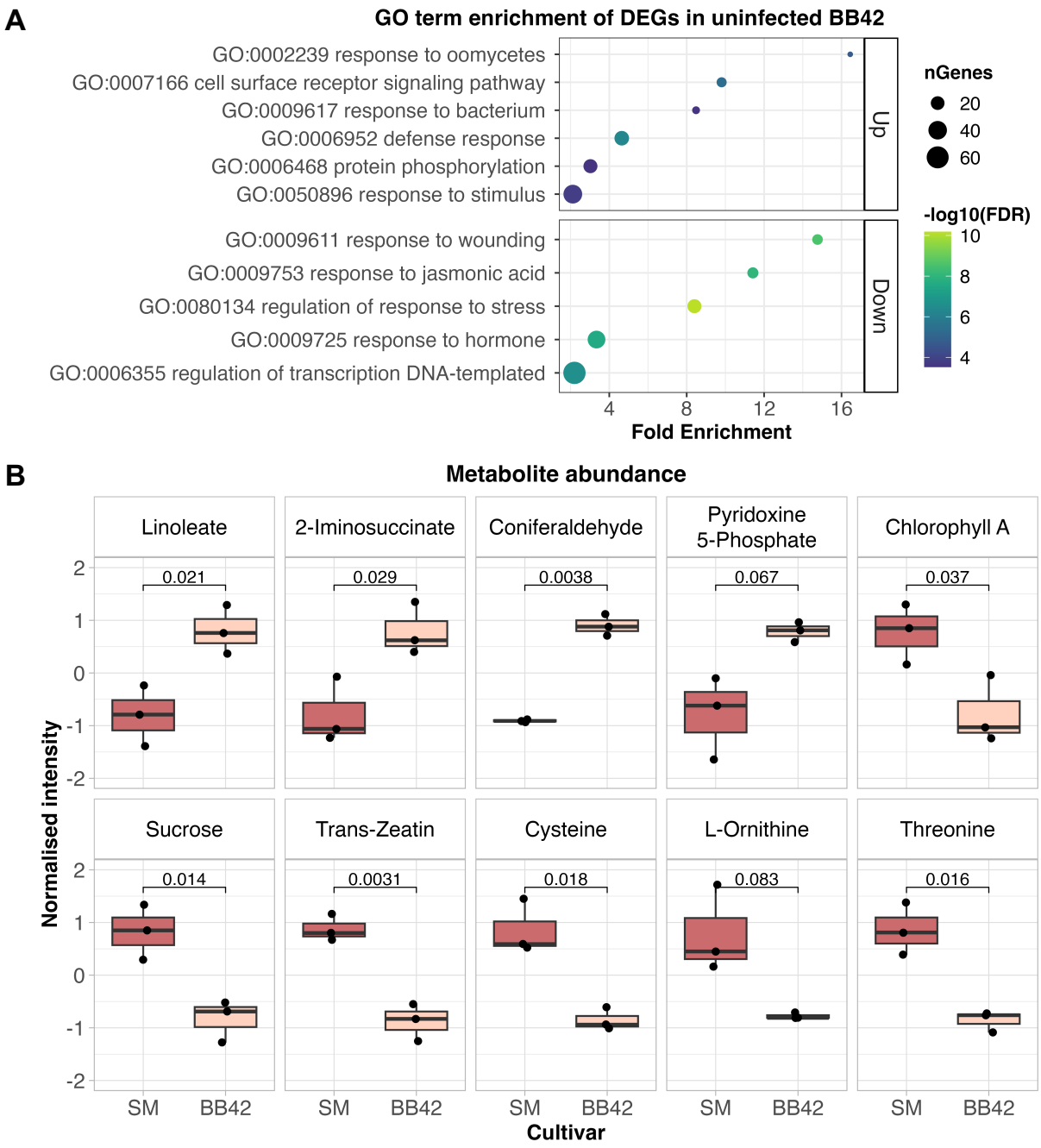

Figure 4: BB42 exhibits constitutive immunity. (A) Gene ontology term enrichment of the genes that are upregulated (top panel) or downregulated (bottom panel) in mock samples of BB42 as compared to the corresponding SM samples. (B) Box plots showing the abundance of certain primary and secondary metabolites that are differentially accumulated between SM and BB42. The raw peak intensities were normalised and plotted on the y-axis. The numbers above the horizontal lines indicate the *P*-values as calculated using unpaired Student's *t*-test considering equal variance between samples. $P<0.05$ is considered statistically significant. Boxes represent the 25th to 75th

percentile while the line within the box indicates the median. The whiskers extend to maximum and minimum data points.

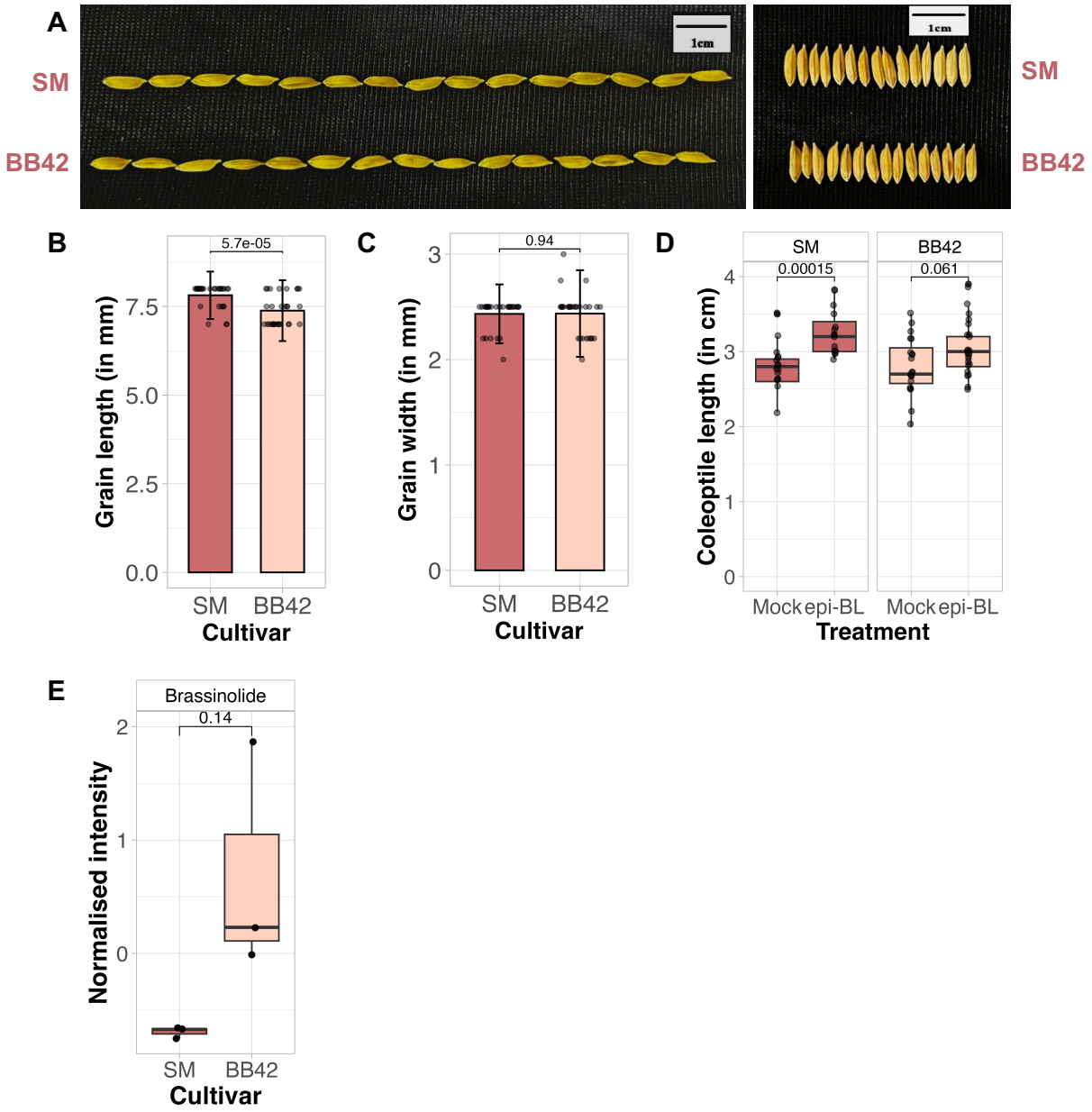

Figure 5: Brassinosteroid signalling is impaired in BB42. (A) Comparison of grain size of SM and BB42. Scale bar = 1 cm. (B) and (C) bar graphs depicting the grain length and grain width, respectively, of SM and BB42. N=30. Bars are drawn to average and the error bars indicate standard deviation. The dots represent the data points. (D) Box plots showing the length of the hypocotyl upon treatment of the seeds with mock solution or solution containing 5µM 24-epibrassinolide. Boxes represent the 25th to 75th percentile while the line within the box indicates the median. The whiskers extend to maximum and minimum data points that are within 1.5 times the interquartile range. Solid black dots outside the whiskers, if any, indicate outliers. N>10. The numbers above the horizontal line indicates *P*-values as calculated using unpaired Student's *t*-test

considering equal sample variance. $P<0.05$ is considered statistically significant. (E) Box plot showing the abundance of brassinolide in SM and BB42 leaves. Boxes represent the 25th to 75th percentile while the line within the box indicates the median. The whiskers extend to maximum and minimum data points.